OFFICE OF NAVAL RESEARCH

TECHNICAL REPORT

FOR

Grant N00014 91 J 1035

R & T Code 413302S - Robert Nowak

Technical Report No. 21

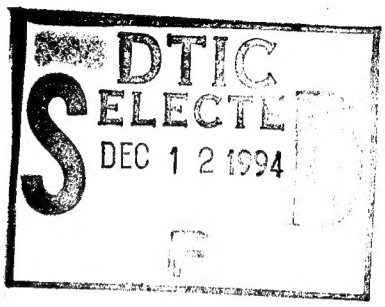

Toward Molecular Selectivity with Chemically Modified Electrodes: Can Electroactivity and Permeability through an Overlaying Metallopolymer Film be Controlled via Rational Manipulation of Internal Architecture?

prepared for publication in J. Electroanal. Chem.

Susan G. Yan and Joseph T. Hupp*
Dept. of Chemistry and Materials Research Center
Northwestern University
Evanston, IL 60208

REPORT DOCUMENTATION PAGE

Form Approved
OMB No. 0704-0188

1. AGENCY USE ONLY (Leave blank)	2. REPORT DATE	3. REPORT TYPE AND DATES COVERED
	Nov. 30, 1994	Technical Report, #21

4. TITLE AND SUBTITLE Toward Molecular Selectivity with chem-Modified Electrodes: Can Electroactivity and Permeability through an Overlaying Metalloplymer Film be Controlled via Rational Manipulation of Internal Architecture?

5. FUNDING NUMBERS
G.N00014-91-J-1035

6. AUTHOR(S)
Susan G. Yan and Joseph T. Hupp

7. PERFORMING ORGANIZATION NAME(S) AND ADDRESS(ES)
Department of Chemistry
Northwestern University
2145 Sheridan Road
Evanston, IL 60208

8. PERFORMING ORGANIZATION REPORT NUMBER
21

9. SPONSORING / MONITORING AGENCY NAME(S) AND ADDRESS(ES)
Office of Naval Research
Chemistry Division
800 North Quincy Ave.
Arlington, VA 22217-500

10. SPONSORING / MONITORING AGENCY REPORT NUMBER

11. SUPPLEMENTARY NOTES
prepared for publication in J. Electroanal. Chem.

12a. DISTRIBUTION / AVAILABILITY STATEMENT

12b. DISTRIBUTION CODE

13. ABSTRACT *(Maximum 200 words)*

Abstract: Metallopolymeric films featuring widely varying metal-to-metal linkage lengths have been prepared via a combination of oxidative and reductive electropolymerization schemes. Each of the film materials exhibits strong size selective permeability behavior towards molecular reactants – providing a primitive physical basis, therefore, for selectivity with respect to reactivity at an underlying electrode. Surprisingly, the observed molecular size cutoffs are essentially independent of film composition, implying that a uniform molecular cavity or pore size exists. Attempts to modify effective pore sizes by introducing large ligand substituents (phenyl groups) at the monomer synthesis stage have failed to alter the pattern of size selectivity. We speculate that: (a) potential pore size expansion effects expected from linkage length extension are offset by enhanced cross linking, and/or (b) electrolyte anion templating effects during film synthesis may be defining the effective minimum pore size, thereby yielding uniform permeation size cutoffs.

14. SUBJECT TERMS	15. NUMBER OF PAGES
	26
	16. PRICE CODE
	UL

17. SECURITY CLASSIFICATION OF REPORT	18. SECURITY CLASSIFICATION OF THIS PAGE	19. SECURITY CLASSIFICATION OF ABSTRACT	20. LIMITATION OF ABSTRACT
unclassified	unclassified	unclassified	UL

INTRODUCTION

One of the objectives of chemical modification of electrode surfaces, particularly for electrocatalytic and sensing applications, is to impart molecular selectivity. Among the simplest approaches to achieving selectivity would be discrimination on the basis of physical size. Indeed, several reports exist wherein size selectivity or "molecular sieving" is achieved via permeation through (or exclusion by) a polymer film containing pores or cavities of a particular molecular size (or size range) [1-7]. We reasoned that selectivity could be systematically tuned if (a) linkage lengths (and presumably, therefore, cavity dimensions) in a cross linked polymer could be systematically varied, and/or (b) monomer substituent sizes (and presumably, therefore, effective cavity volumes) in the same or similar polymers could likewise be varied. We report here the results of our efforts to control selectivity via both strategies.

The system selected was a metallopolymer coating on platinum with primarily ferrocene species as permeants. The particular choice of polymer was one derived from ruthenium complexes of 1,10-phenanthroline (phen) and any of several bipyridines, where one of the nitrogens of each of two bipyridine ligands (L) remains uncoordinated in the monomeric compound. We have previously shown that these complexes rapidly polymerize following electrochemical oxidation of the metal center [8,9]. (For a related report, see Calvert, et al. [10].) When the oxidation is carried out by cyclic voltammetry, adherent electrode film coatings are obtained that retain the electrochemical properties of the monomeric precursors. The mechanism of polymerization appears to involve nucleophilic attack of phenanthroline by the free pyridyl nitrogen, where attack is activated by ruthenium oxidation. In any case, crystallographic studies of related monomeric reaction products (unpublished) have established

that the linkage structure (for L=4,4'-bipyridine) is the following [11]:

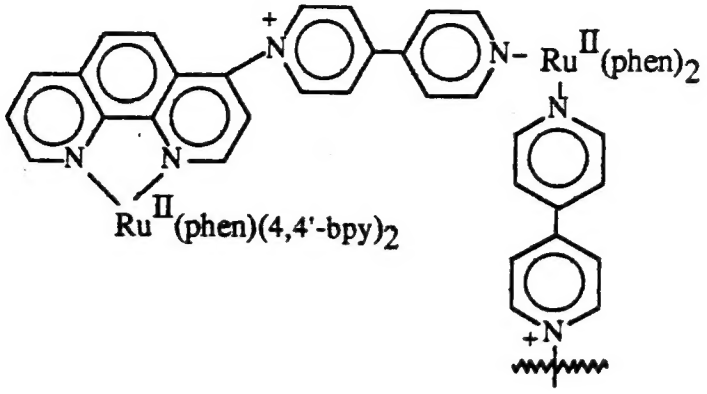

We reasoned that linkage lengths could be arbitrarily manipulated by replacing 4,4'-bipyridine with ligands featuring hydrocarbon spacers between the pyridyl rings. Alternatively, metallopolymers featuring shorter linkages of a slightly different form can be obtained via oxidative or reductive activation, respectively, of $Fe(5\text{-amino-}1,10\text{-phenanthroline})_3^{2+}$ [12] or $Ru(5\text{-chloro-}1,10\text{-phenanthroline})_3^{2+}$ [13], as sketched below:

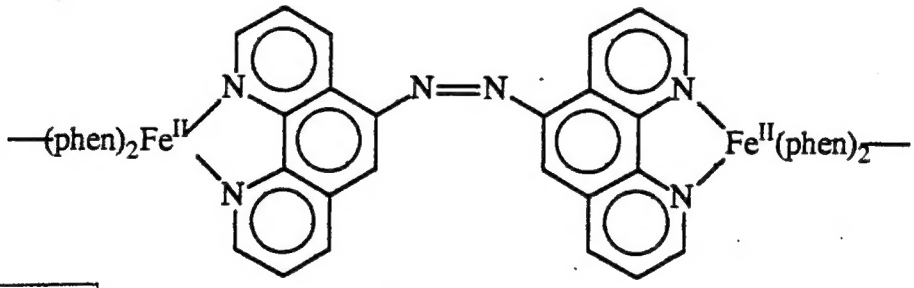

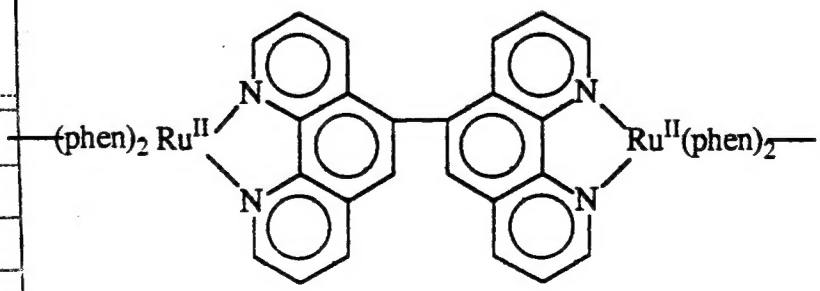

Finally, we reasoned that with electroactive permeants such as ferrocene, permeation (and therefore, selectivity) could be quantitatively assessed by monitoring transient and steady state oxidation currents at the underlying electrode, as in previous investigations [1-7].

EXPERIMENTAL

Materials. $RuCl_3$ was purchased from Aesar. 1,10-phenanthroline, 5-chloro-1,10-phenanthroline (Cl-phen) and 5-phenyl-1,10-phenanthroline (phenyl-phen) were purchased from GFS Chemicals. (Ligand structures are shown in Figure 1.) 5-amino-1,10-phenanthroline (NH_2-phen) was purchased from Polysciences. 4,4'-bipyridine (4,4'-bpy), 1,2-bis(4-pyridyl)ethylene (BPE), 1,2-bis(4-pyridyl)ethane (BPA) and 4,4'-trimethylenedipyridine (TMP) were purchased from Aldrich Chemical Co. Reagent grade acetonitrile and dichloromethane were purchased from Fisher and distilled from CaH_2 prior to use. Tetrabutylammonium perchlorate (TBAP) (GFS Chemicals) was recrystallized in purified distilled water and dried *in vacuo*.

ß,ß'-bis(4-pyridyl)-1,4-diethylbenzene (BPEB) was prepared as follows. 0.0103 mol lithium diisopropylamide (prepared from diisopropylamine and butyllithium in 10 ml distilled tetrahydrofuran (THF) under N_2) was added dropwise to 1.0 ml distilled 4-picoline in 100 ml THF in an acetone/dry ice bath and stirred for 20 minutes. 1.36 g (5.15×10^{-3} mol) of α,α'-dibromo-p-xylene (purified by recrystallization from hot methanol) was dissolved in 50 ml THF and added dropwise to the orange 4-picoline solution. The mixture was stirred overnight under N_2 whereupon it turned light pink. 100 ml of $NaCl/H_2O$ was added. THF was evaporated and a tan compound precipitated. This material (crude product) was then removed

by extraction into distilled dichloromethane. After evaporation of the dichloromethane, a yellow semicrystalline residue was collected. The residue was purified by recrystallization from ethyl acetate. *Anal. calcd. (found):* C, 82.86 (83.30), H, 7.23 (6.99), N, 9.60 (9.71). ^{1}H NMR ($CDCl_3$): d 8.5 (4H), 7.06 (8H), 2.9 (8H). Mass spectrometry: m/e = 287, 196, 104.

Permeants. Several ferrocene species were purchased from Aldrich Chemical Co. (either Aldrich's standard catalog listing or the Sigma-Aldrich Library of Rare Chemicals). $Fe(vbpy)_2(CN)_2$ was synthesized via literature methods [14,15]. Structures of the permeants are shown in Figure 2.

Polymer precursors. $[Fe(NH_2\text{-phen})_3](PF_6)_2$ and $[Ru(Cl\text{-phen})_3](PF_6)_2$ were prepared by published methods [12,13]. The various $[Ru(5\text{-R-phen})_2L_2](PF_6)_2$ (R=H or phenyl; L=4,4'-bpy, BPE,BPA,TMP or BPEB) species were prepared and purified by a general literature method [16]. Several of these compounds have been reported previously [8, 9]. For new compounds the following elemental analysis data were obtained. *Anal. calcd. (found) for* $[Ru(phen)_2(BPEB)_2](PF_6)_2$*:* C, 55.34 (57.88), H, 4.29 (4.25), N, 7.75 (8.44). *Anal. calcd. (found) for* $[Ru(5\text{-phenyl-phen})_2(4,4'\text{-bpy})_2](PF_6)_2 \cdot H_2O$*:* C, 54.60 (54.51), H, 3.40 (3.43), N, 8.77 (9.08). *Anal. calcd. (found) for* $[Ru(5\text{-phenyl-phen})_2(TMP)_2](PF_6)_2 \cdot 3H_2O$*:* C, 54.57 (54.01), H, 4.00 (3.99), N, 8.36 (8.54)

Measurements. Cyclic voltammetry measurements were made by using a Princeton Applied Research polarographic analyzer (Model 264A) and a Houston Instruments X-Y recorder (Model 2000). For rotating disk electrode (RDE) measurements, a Pine Instruments Analytical Rotator (Model MSRX) was also employed. Electrochemical measurements were made in standard two compartment cells containing 0.1 *M* TBAP in acetonitrile (or occasionally

dichloromethane; see below) as solvent. The cells featured a platinum disk working electrode (1 mm diameter), a platinum wire counter electrode and a saturated (sodium chloride) calomel reference electrode (s.s.c.e.).

RESULTS AND DISCUSSION

Metallopolymer synthesis. As suggested by the growth cycles in Figure 3, adherent films of *poly*-$Ru(phen)_2L_2^{n+}$ were readily prepared from ca. 1 mM solutions of monomer via repetitive voltammetry (100 mV/s) between 0.70 and 1.70 V (i.e., the Ru(II/III) region). For $Ru(phen)_2(4,4'\text{-bpy})_2^{2+}$, $Ru(phen)_2(BPA)_2^{2+}$, $Ru(phen)_2(BPE)_2^{2+}$, and $Ru(phen)_2(TMP)_2^{2+}$, films proved accessible from acetonitrile as the polymerization medium. For $Ru(phen)_2(BPEB)_2^{2+}$, $Ru(5\text{-phenyl-phen})_2(4,4'\text{-bpy})_2^{2+}$ and $Ru(5\text{-phenyl-phen})_2(TMP)_2^{2+}$, however, polymeric films were obtained only from dichloromethane. Independent of the medium for polymerization, the series of films uniformly exhibited stable metal-centered electrochemical responses in monomer-free solutions. Film thicknesses could be estimated, therefore, by integrating the responses and utilizing Faraday's law. (Effective monomer dimensions of ca. 15 x 15 x 15 Å were assumed in thickness calculations. Calculated metal-to-metal separation distances through fully extended linkages range from 11 to 23 Å.)

Permeation: general studies. Figure 4 shows representative voltammograms for ferrocene and dibenzoylferrocene containing solutions at bare (top panel) and *poly*-$Ru(phen)_2(TMP)_2^{n+}$-coated (bottom panel) electrodes (stationary electrodes). The comparison clearly shows that the polymer coated electrode selectively responds to ferrocene, the smaller of the two reactants. Additionally, the response at the coated electrode is distorted

in a manner that is strongly suggestive of mass transport inhibition by slow diffusion (permeation) through a barrier layer (i.e., the metallopolymer).

To place the studies on more quantitative grounds, we employed rotating disk electrode voltammetry. Under these conditions, the limiting rate (or current, i_{lim}) for solute oxidation necessarily depends on both the rate of mass transport (forced convection) through the solution phase and the rate of permeation through the polymer film. If these are viewed as consecutive rate processes then [4]:

$$i_{lim}^{-1} = i_{mass\ transport}^{-1} + i_{permeation}^{-1} \quad (1)$$

The individual terms are further defined as [4]:

$$i_{mass\ transport} = 0.620nFAD^{2/3}\omega^{1/2}\nu^{-1/6}C_{soln} \quad (2)$$

$$i_{permeation} = nFAPD_{film}C_{soln}/d \quad (3)$$

where ω is the rotation rate, ν is the kinematic viscosity, n is the number of electrons transferred per permeant, F is the Faraday, A is the electrode area, C_{soln} is the solute concentration, and d is the polymer film thickness. The permeability, PD_{film}, is the product of the solute partition coefficient (P) and its diffusion coefficient (D_{film}) within the film.

As suggested by eqs 1-3, the effects of convection and permeation can be separated by measuring the overall rate of solute oxidation as a function of electrode rotation rate. Figure 5 shows a plot of i_{lim}^{-1} versus $\omega^{-1/2}$ for ferrocene oxidation at a *poly*-Ru(phen)$_2$(TMP)$_2^{n+}$-coated electrode. From the intercept, $i_{permeation}$ is 19 μA and PD_{film} is 2.1 x 10^{-8} cm^2/s. An additional experiment in which $i_{permeation}$ was measured as a function of inverse film thickness (Figure 6; eq.3) confirms that film-based transport indeed does occur by permeation rather than, for example, pinhole diffusion.

Permeant dependence. To explore the issue of selectivity – especially molecular sieving – we additionally examined permeation as a function of permeant size. To avoid complications from either electrostatic enhancement of partitioning or Donnan exclusion, we limited our study to neutral permeants. As indicated by Figure 2, the majority of the permeants were ferrocene species, where size variations were achieved by varying the identities and, therefore, sizes of substituents. Because many of the permeants are irregularly shaped, however, a fully satisfactory description of relative sizes was difficult to establish. We ultimately chose to employ the solution-phase diffusion coefficient as a reasonably objective *inverse* measure of effective molecular size. (Recall that for spherical molecules, the Stokes-Einstein equation predicts an inverse relationship between D and the molecular radius. Koval and co-workers have additionally established that the inverse radius relationship holds reasonably well for *non*spherical molecules if geometrically averaged radii are employed [17].)

Figure 7 shows a plot of permeability versus D (i.e. relative inverse molecular size) for eight neutral permeants in a *poly*-$Ru(phen)_2(4,4'\text{-}bpy)_2^{n+}$ film. The most striking feature is the sharp cutoff of permeability with increasing permeant size (cf. Fig. 3). The behavior is reminiscent of prior correlations of permeability with molecular *volume* for vinyl(bi)pyridine-based metallopolymer films [1,3-5] and is suggestive of a relatively narrow distribution of film pore or cavity sizes. (Residual signals for the largest molecules are probably indicative of pinhole diffusion rather than true permeation.)

Film structure dependence. With the behavior of intermediate linkage (i.e., 4,4'-bpy based) films established, we sought to examine films with both longer and shorter links. Our expectation was that permeation and size-based selectivity would be modified in ways that

reflected the anticipated increases and decreases, respectively, in polymer pore size. Figure 8 shows plots of permeability versus D for phen-based films featuring TMP and BPEB linkages ("long linkages"; see Fig. 1). Figure 9, on the other hand, presents data for films derived from $Ru(Cl\text{-}phen)_3^{2+}$ (*direct* linkage of phenanthroline ligands) and $Fe(NH_2\text{-}phen)_3^{2+}$ (probable N=N links between phen ligands) ("short linkages"). Each of the six additional films displays sharp molecular sieving behavior. Surprisingly, however, the molecular size cutoff (as indicated by D) is virtually the same for each film – this despite calculated metal-metal separation distances that vary from ~23 Å ($Ru(phen)_2(BPEB)_2^{2+}$-based films) to ~11 Å ($Ru(5\text{-}Cl\text{-}phen)_3^{2+}$-based films)!

Given the failure of fairly extensive linkage length variations to induce significant changes in molecular selectivity, we attempted to modulate selectivity by altering the metallopolymer architecture in a different way. Specifically, we attempted to diminish effective cavity volumes, for fixed linkage lengths, by introducing a phenyl substituent at the 5 site of 1,10-phenanthroline in both *poly*-$Ru(R\text{-}phen)_2(4,4\text{-}bpy)_2^{n+}$ and *poly*-$Ru(R\text{-}phen)_2(TMP)_2^{n+}$ films. The resulting permeation behavior is shown in Figures 10 and 11. Remarkably, the phenyl-containing films display size selectivities that are essentially identical to those shown in Figures 7-9.

The appearance of a seemingly universal polymer-based cavity or pore size, corresponding approximately to the dimensions of dimethylferrocene, is both surprising and puzzling. We speculate that the near constancy reflects a compensation between effects associated with linkage length (where longer lengths obviously should favor larger pore sizes) and degree of cross linking (where greater cross linking should yield smaller pore sizes). If

longer linkage ligands yield significant steric advantages with respect to cross linking efficiency, the net effect might be the observed linkage independence of the effective pore size.

Alternatively (or additionally) the constancy implied by Figures 7-11 might be indicative of a templating effect. Film growth from cationic monomers requires intimate association with, and ultimately incorporation of, charge compensating anions. With the possible exception of the synthesis involving $Ru(5\text{-}Cl\text{-}phen)_3^{2+}$ (where chloride ions may be incorporated [13]), film growth requires participation specifically of the electrolyte based perchlorate ions. Presumably the anion imposes a minimum pore/cavity size corresponding approximately to its diameter (~4.2 Å) or volume (~39 $Å^3$). For comparison, the approximate diameter of ferrocene is 4.8 Å (major axis); the approximate van der Waals volume is 68 $Å^3$.

If the second explanation is correct (or partially correct) it suggests that the initial goal of controlling permeant selectivity by manipulating effective metallopolymer pore sizes might be achievable by varying the electrolyte anion size [18]. Alternatively, a (secondary) crosslinking reaction *after* film formation [19] might provide a viable route to cavity/pore size modulation and varied permeant selectivity.

CONCLUSIONS

Metallopolymeric films featuring widely varying metal-to-metal linkage lengths can be prepared via a combination of oxidative and reductive electropolymerization schemes. All of the films exhibit size selective permeability behavior towards molecular reactants. Surprisingly, however, the molecular size cutoff is independent of film composition — implying that films with widely varying metal-to-metal linkage lengths nevertheless contain pores of very similar size. Attempts to diminish effective pore sizes by introducing large ligand substituents (phenyl

groups) at the monomer synthesis stage were unsuccessful, at least as judged by subsequent film permeation studies. We speculate that the potential pore-size expansion effects expected from linkage length extension are compensated by enhanced cross linking. Alternatively (or additionally) the near constancy of effective pore sizes may be indicative of an electrolyte anion templating effect during film formation.

REFERENCES

1. S. Gould, T. J. Meyer, *J. Am. Chem. Soc.*, **113**, 7442 (1991).
2. T. Ohsaka, T. Hirokawa, H. Miyamoto, N. Oyama, *Anal. Chem.* **59**, 1758 (1987).
3. A. G. Ewing, B. J. Feldman, R. W. Murray, *J.Phys.Chem.*, **89**, 1263, (1985).
4. T. Ikeda, R. Schmehl, P. Denisevich, K. Willman, R. W. Murray, *J. Am. Chem. Soc.* **104**, 2683 (1982).
5. S. Gould, G. F. Strouse, T. J. Meyer, B. P. Sullivan, *Inorg. Chem.*, **30**, 2942 (1991).
6. K. A. Pressprich, S. G. Maybury, R. E. Thomas, R. W. Linton, E. A. Irene, R. W. Murray, *J. Phys. Chem.*, **93**, 5568 (1989).
7. R. L. McCarley, E. A. Irene, R. W. Murray, *J. Phys. Chem.*, **93**, 5568 (1989).
8. O. Fussa-Rydel, J. T. Hupp, *J. Electroanal. Chem.*, **251**, 417 (1988).
9. H. T. Zhang, P. Subramanian, O. Fussa-Rydel, J.C. Bebel, J.T. Hupp, *Solar Energy Mater. Solar Cells*, **25**, 315 (1992).
10. J. M. Calvert, D. L. Peebles, R. J. Nowak, *Inorg. Chem.*, **24**, 3111 (1985).
11. L. Skeens-Jones, J.A. Ibers, P. Subramanian, J.T. Hupp, unpublished studies.
12. C.D. Ellis, L.D. Margerum, R.W. Murray, T. J. Meyer, *Inorg. Chem.*, **22**, 1283 (1989).

13. O. Fussa-Rydel, H. T. Zhang, J.T. Hupp, C.R. Leidner, *Inorg. Chem.*, **28,** 1533 (1989).

14. H. D. Abruña, A. I. Breikss, D.B. Collum, *Inorg. Chem.*, **24**, 987 (1985).

15. A. A. Schilt, *J. Am. Chem. Soc.*, **82**, 3000 (1960).

16. J. M. Calvert, R. H. Schmehl, B. P. Sullivan, J. S. Facci, T. J. Meyer, R. W. Murray, *Inorg. Chem.*, **22**, 2151 (1983).

17. C. A. Koval, M.E. Ketterer, C. M. Reidsema, *J. Phys. Chem.*, **90**, 4201 (1985).

18. S. Cosnier, A. Deronzier, J.-F. Roland, *J. Electroanal. Chem.* **310**, 71 (1991).

19. R. L. McCarley, R. E. Thomas, E. A. Irene, R. W. Murray, *J. Electroanal. Chem.* **290**, 79 (1990).

FIGURE CAPTIONS

1. Ligand structures and abbreviations.

2. Permeant structures: (a) $Fe(vbpy)_2(CN)_2$, (b) 1,1'-bis(diphenylphosphino)ferrocene, (c) *t*-butyl-3-ferrocenylmethylene carbazate, (d) 1,1'-biferrocene, (e) N-ferrocenylmethylene-4-phenylazo aniline, (f) 1,1'-dibenzoylferrocene, (g) 1,1'-dimethylferrocene, (h) ferrocene.

3. Consecutive voltammograms for oxidative growth of a *poly*-$Ru(phen)_2(TMP)_2^{n+}$ film on a platinum disk in acetonitrile.

4. Stationary voltammograms (100 mV/s) for an acetontrile solution containing ferrocene (E_f = 400 mV) and dibenzoylferrocene (E_f = 880 mV). Panel *A*: bare platinum electrode. Panel *B*: *poly*-$Ru(phen)_2(TMP)_2^{n+}$ coated platinum electrode.

5. Rotating disk voltammetry: i_{lim}^{-1} versus $\omega^{-1/2}$ for ferrocene oxidation at a *poly*-$Ru(phen)_2(TMP)_2^{n+}$ coated electrode.

6. Dependence of $i_{permeation}$ (eq. 3) for ferrocene oxidation on reciprocal thickness (d^{-1}) of *poly*-$Ru(phen)_2(TMP)_2^{n+}$ based films.

7. Permeation rate, PD_{film}, versus solution phase diffusion coefficient for a series of molecular permeants (see caption to Figure 2 for key). Film composition is *poly*-$[Ru(phen)_2(4,4'\text{-}bpy)_2](ClO_4)_n$.

8. Permeation rate, PD_{film}, versus solution phase diffusion coefficient for a series of molecular permeants (see caption to Figure 2 for key). Panel *A*: *poly*-$[Ru(phen)_2(TMP)_2](ClO_4)_n$ film. Panel *B*: *poly*-$[Ru(phen)_2(BPEB)_2](ClO_4)_n$ film.

9. Permeation rate, PD_{film}, versus solution phase diffusion coefficient for a series of molecular permeants (see caption to Figure 2 for key). Panel *A*: film derived from

$Ru(Cl\text{-}phen)_3^{2+}$. Panel *B*: film derived from $Fe(NH_2\text{-}phen)_3^{2+}$.

10. Permeation rate, PD_{film}, versus solution phase diffusion coefficient for a series of molecular permeants (see caption to Figure 2 for key). Film composition is *poly*-$[Ru(phenyl\text{-}phen)_2(4,4'\text{-}bpy)_2](ClO_4)_n$.

11. Permeation rate, PD_{film}, versus solution phase diffusion coefficient for a series of molecular permeants (see caption to Figure 2 for key). Film composition is *poly*-$[Ru(phenyl\text{-}phen)_2(TMP)_2](ClO_4)_n$.

4,4'-bpy 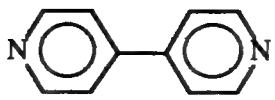

BPA 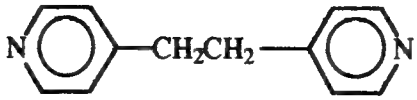

BPE 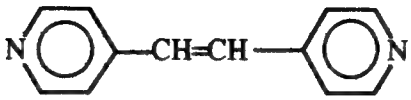

TMP 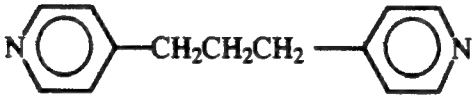

BPEB 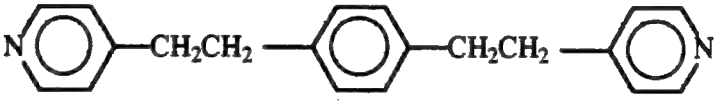

phen 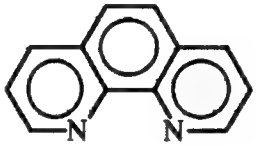

NH_2-phen 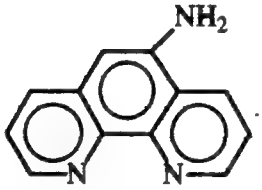

Cl-phen 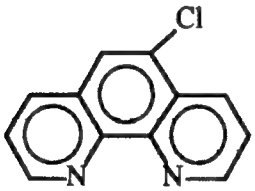

phenyl-phen 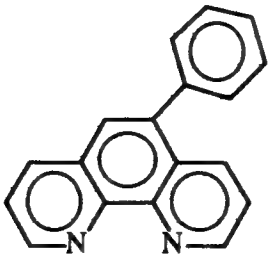

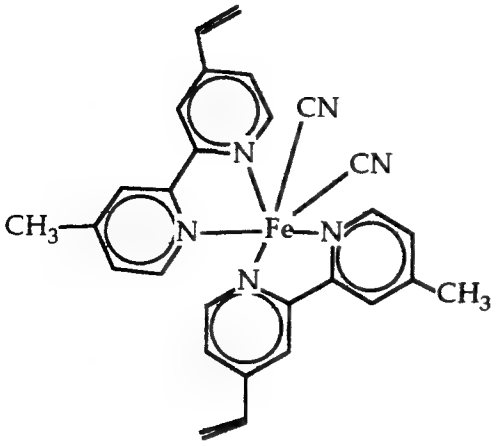
CN
CN
N
N
Fe
N
N
CH_3
CH_3

(a)

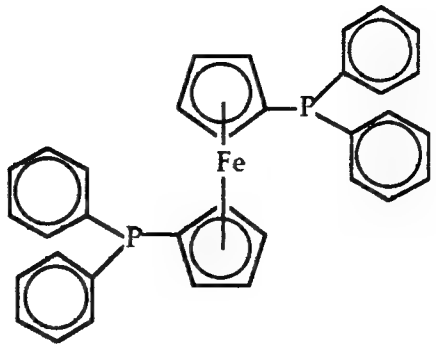
P
Fe
P

(b)

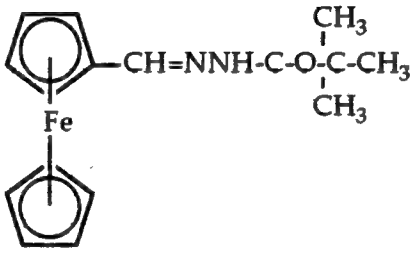
CH_3
CH=NNH-C-O-C-CH_3
CH_3
Fe

(c)

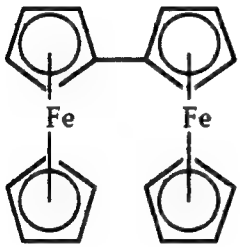
Fe
Fe

(d)

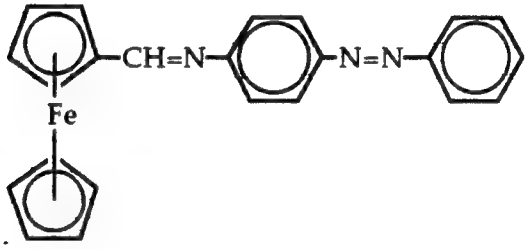
CH=N
N=N
Fe

(e)

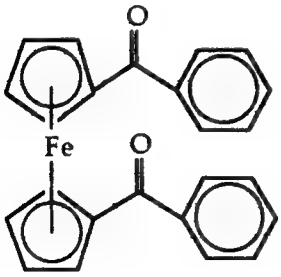
O
Fe
O

(f)

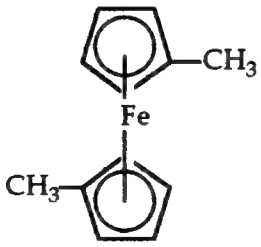
CH_3
Fe
CH_3

(g)


Fe

(h)

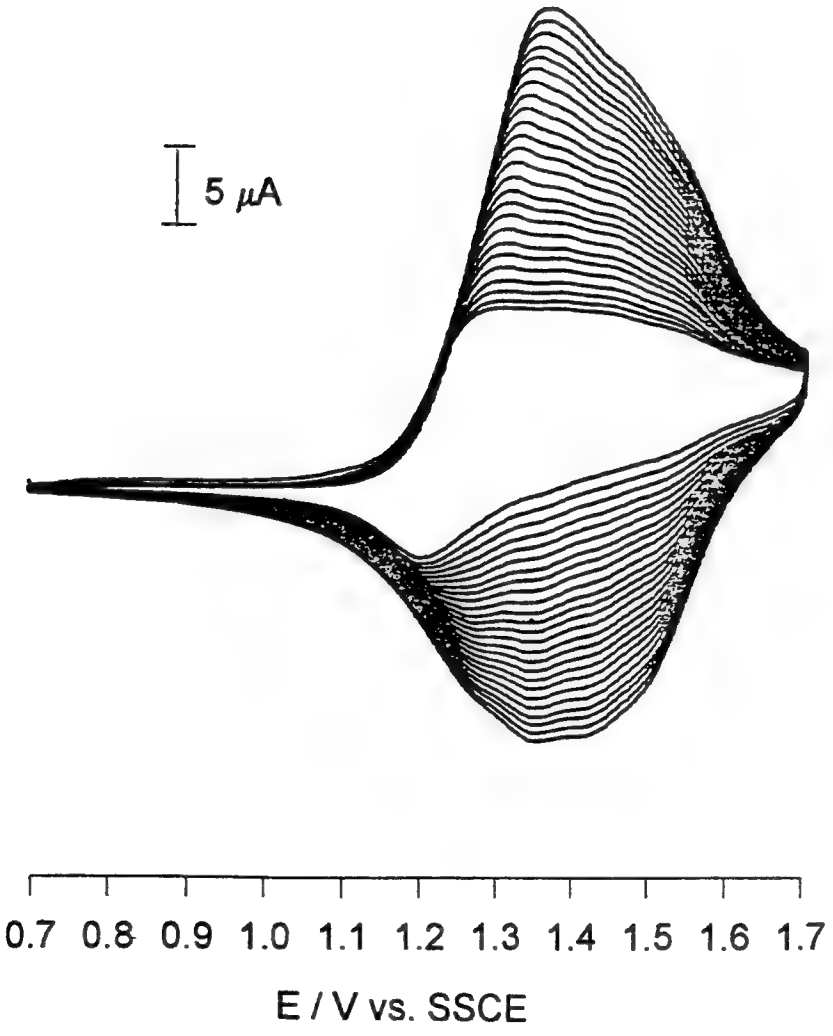

Fig 3

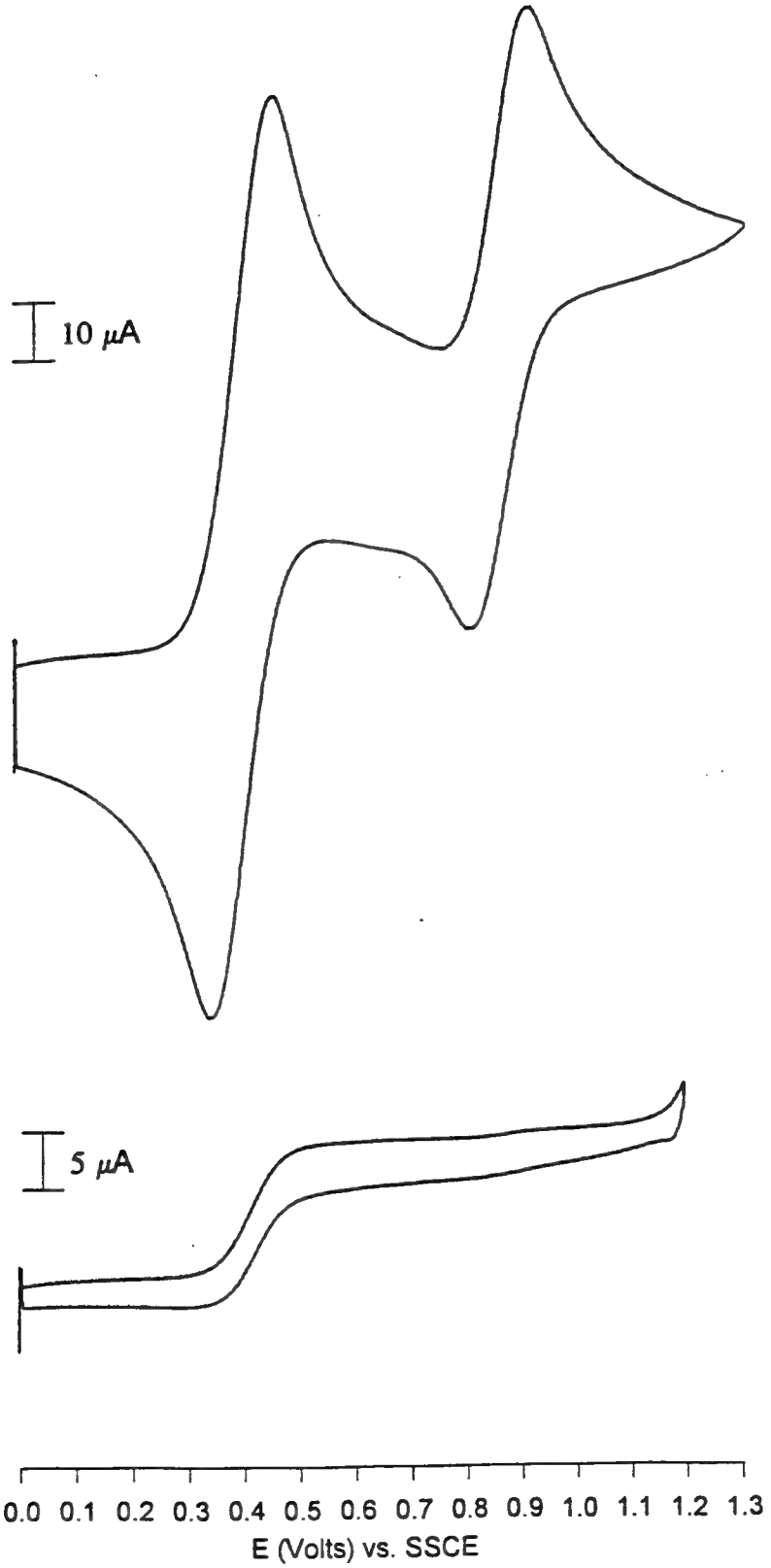
10 μA
5 μA
0.0 0.1 0.2 0.3 0.4 0.5 0.6 0.7 0.8 0.9 1.0 1.1 1.2 1.3
E (Volts) vs. SSCE

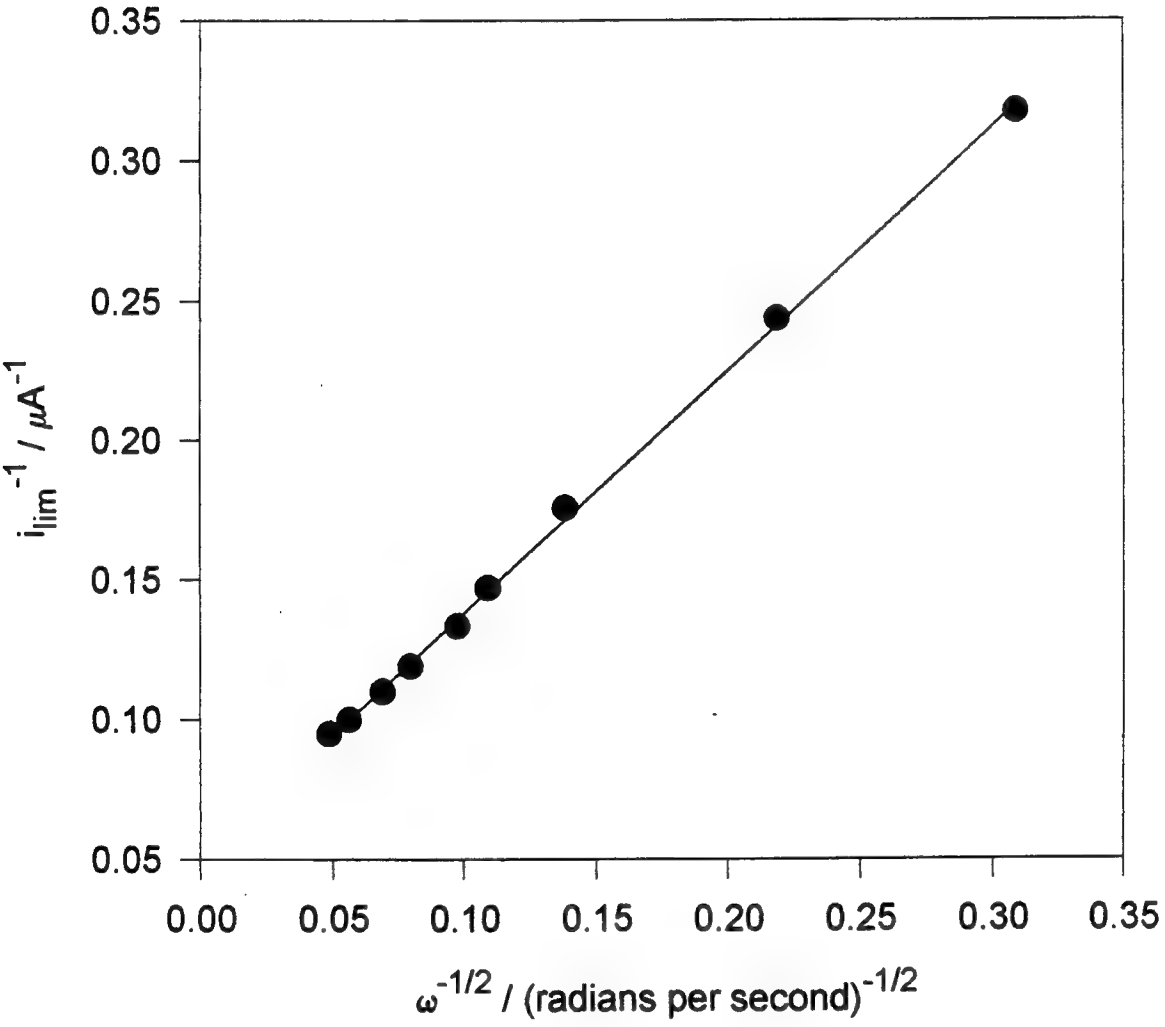
0.35
0.30
0.25
0.20
0.15
0.10
0.05
i_{lim}^{-1} / μA^{-1}
0.00
0.05
0.10
0.15
0.20
0.25
0.30
0.35
$\omega^{-1/2}$ / (radians per second)$^{-1/2}$

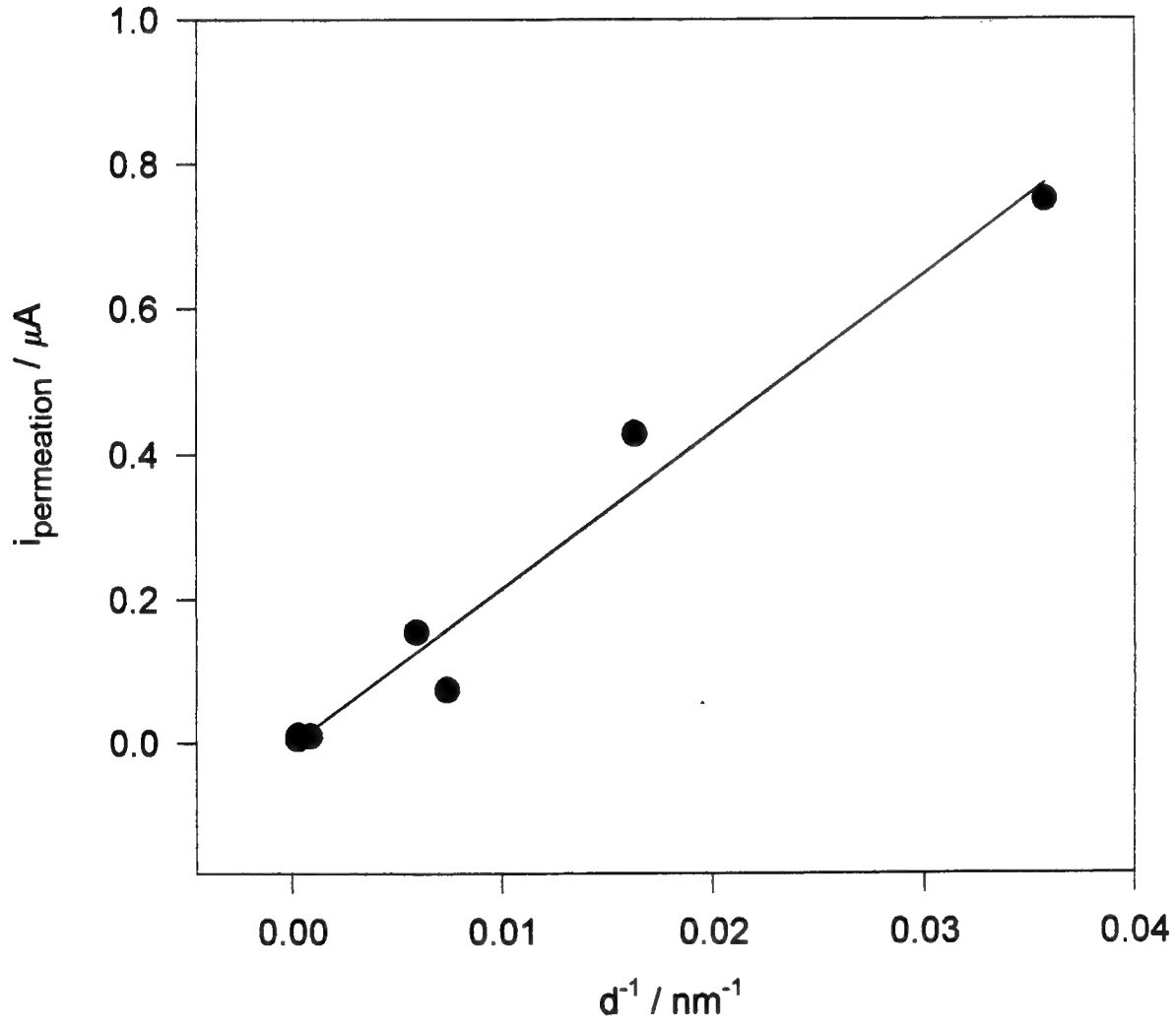
1.0
0.8
0.6
0.4
0.2
0.0
$i_{permeation}$ / μA
0.00
0.01
0.02
0.03
0.04
d^{-1} / nm^{-1}

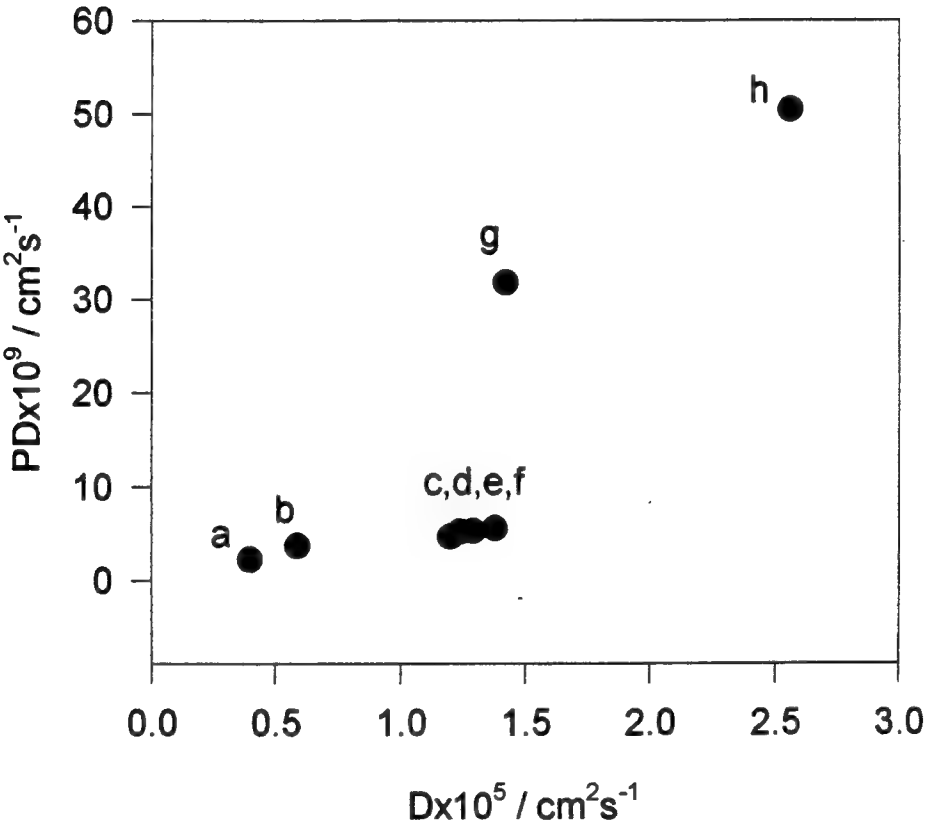
60
50
40
30
20
10
0
PDx10^9 / cm^{2}s^{-1}
h
g
c,d,e,f
b
a
0.0
0.5
1.0
1.5
2.0
2.5
3.0
Dx10^5 / cm^{2}s^{-1}

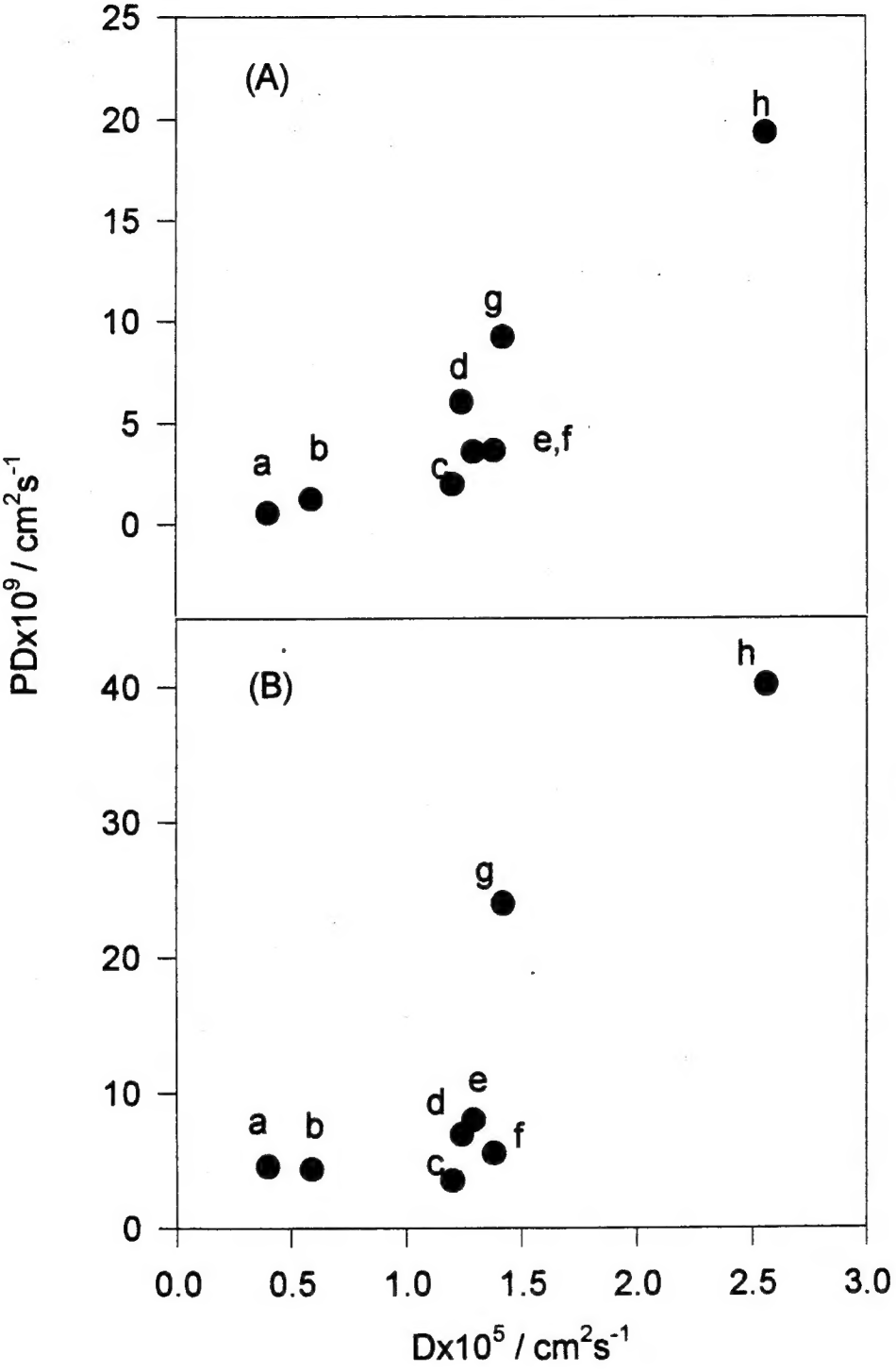
(A)
(B)
h
g
d
e,f
a
b
c
e
f
PDx10^9 / cm^2s^-1
Dx10^5 / cm^2s^-1
0
5
10
15
20
25
30
40
0.0
0.5
1.0
1.5
2.0
2.5
3.0

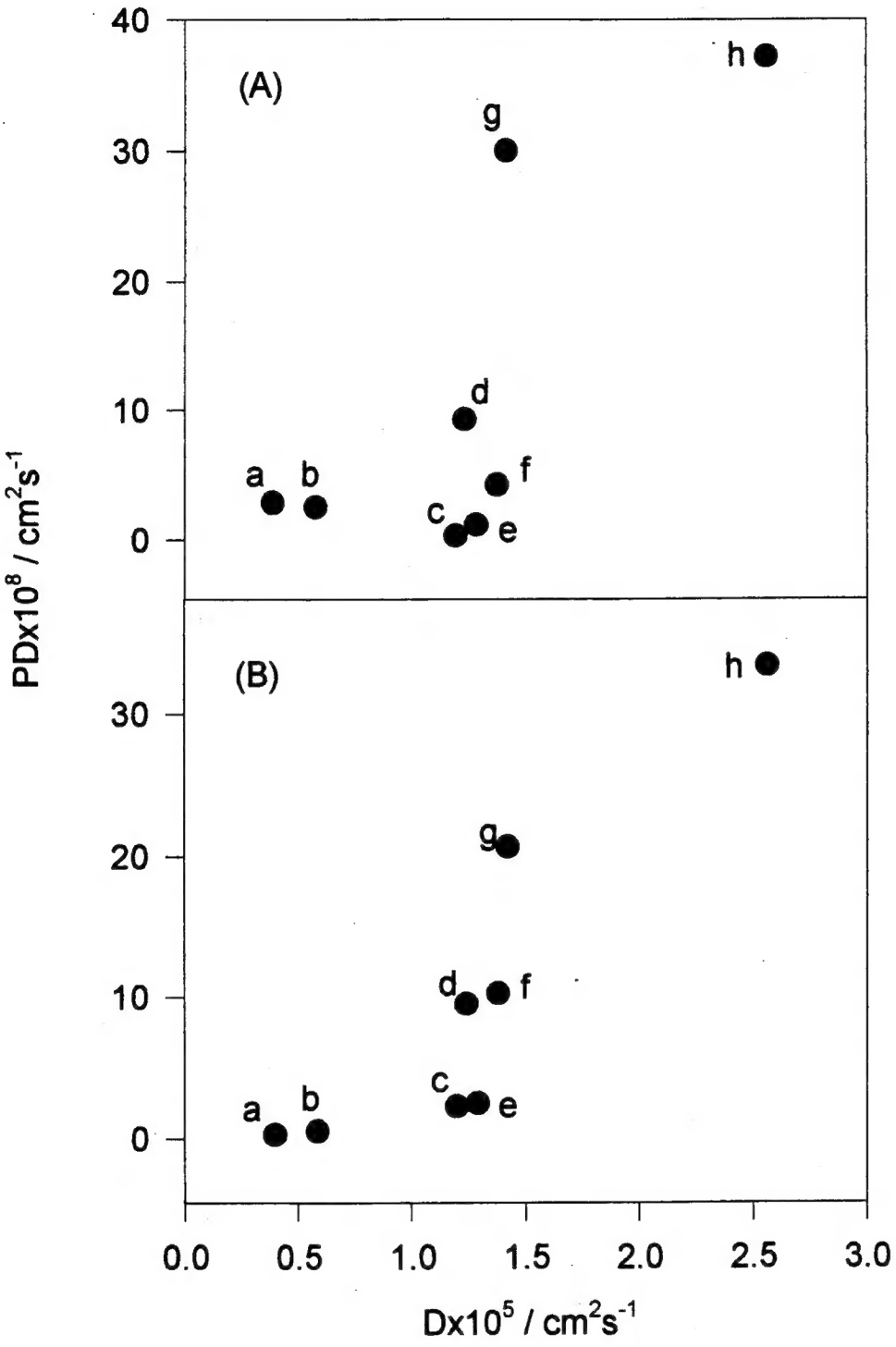
(A)
(B)
h
g
d
f
a
b
c
e
40
30
20
10
0
0.0
0.5
1.0
1.5
2.0
2.5
3.0
PDx10^8 / cm^2s^-1
Dx10^5 / cm^2s^-1

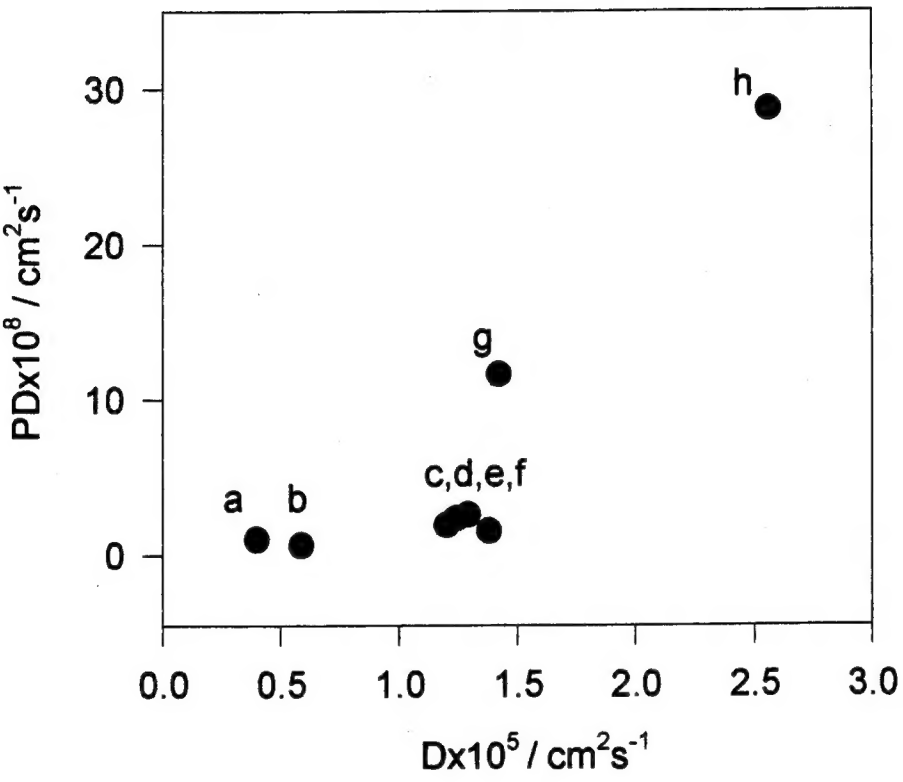
30
20
10
0
PDx10^8 / cm^2s^-1
h
g
c,d,e,f
a
b
0.0
0.5
1.0
1.5
2.0
2.5
3.0
Dx10^5 / cm^2s^-1

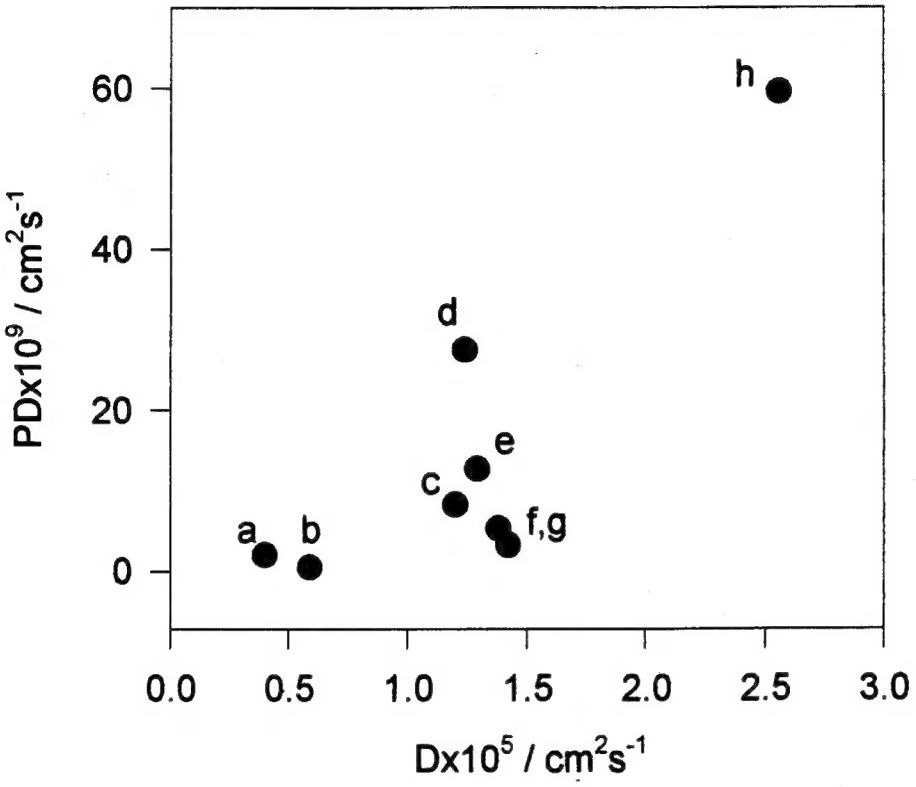
60
40
20
0
PDx10^9 / cm^2s^-1
h
d
e
c
a
b
f,g
0.0
0.5
1.0
1.5
2.0
2.5
3.0
Dx10^5 / cm^2s^-1